

DisCa: Accelerating Video Diffusion Transformers with Distillation-Compatible Learnable Feature Caching

Chang Zou^{1,2}, Changlin Li², Yang Li², Patrol Li², Jianbing Wu², Xiao He^{2,3},
Songtao Liu², Zhao Zhong², Kailin Huang¹, Linfeng Zhang¹ *

¹Shanghai Jiao Tong University ²Tencent Hunyuan ³Xidian University

Abstract

While diffusion models have achieved great success in the field of video generation, this progress is accompanied by a rapidly escalating computational burden. Among the existing acceleration methods, Feature Caching is popular due to its training-free property and considerable speedup performance, but it inevitably faces semantic and detail drop with further compression. Another widely adopted method, training-aware step-distillation, though successful in image generation, also faces drastic degradation in video generation with a few steps. Furthermore, the quality loss becomes more severe when simply applying training-free feature caching to the step-distilled models, due to the sparser sampling steps. This paper novelly introduces a distillation-compatible learnable feature caching mechanism for the first time. We employ a lightweight learnable neural predictor instead of traditional training-free heuristics for diffusion models, enabling a more accurate capture of the high-dimensional feature evolution process. Furthermore, we explore the challenges of highly compressed distillation on large-scale video models and propose a conservative Restricted MeanFlow approach to achieve more stable and lossless distillation. By undertaking these initiatives, we further push the acceleration boundaries to 11.8× while preserving generation quality. Extensive experiments demonstrate the effectiveness of our method. The code is in the supplementary materials and will be publicly available.

1. Introduction

In recent years, Diffusion Models (DMs) [15, 16, 58] have achieved remarkable success in the generative domain, including but not limited to modalities such as image [24, 50], video [1, 3, 23, 64, 65], audio [8, 10], and text [46, 80] generation. To further enhance generation quality, the scale of

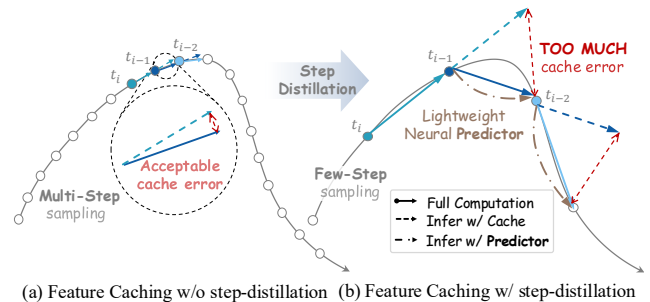


Figure 1. **Feature Caching on the diffusion sampling process w/ and w/o step-distillation.** (a) Adjacent timesteps are similar under the undistilled models, allowing traditional caching with simple reuse/interpolation. (b) Significant inter-step differences cause traditional caching to fail; the proposed learnable predictor captures the high-dimensional feature evolution successfully.

DMs has been rapidly increasing [28, 63, 66, 68], accompanied by a continuous rise in their computational load, making the deployment costs of these models prohibitively high.

To address this issue, numerous acceleration methods have been proposed [36, 71, 72, 75, 83], primarily focusing on Sampling Timestep Reduction and Denoising Network Acceleration. Among these, training-aware step distillation [14, 69, 70] and training-free feature caching methods [13, 31, 43] have demonstrated superior performance and have been widely adopted, respectively.

Recently, MeanFlow [14], as one of the representative methods in step-distillation, builds upon prior research [12, 36] with a breakthrough by shifting the sampling objective of DMs from instantaneous velocity to average velocity.

However, when applied to distill *highly complex large video generation models* [22, 65], the numerical errors led by its differentiation operations (i.e., Jacobian-vector product (JVP) operations), coupled with MeanFlow’s inherently too aggressive design for one-step distillation, can result in catastrophic training divergence and generative artifacts.

Traditional training-free feature caching methods primarily accelerate computation by caching and reusing all [25, 31, 41] or partial [19, 42, 43, 83] previously com-

*Corresponding Author.

puted features, thereby skipping relatively non-critical computations. However, since the features at adjacent timesteps in DMs are inherently different, this approach inevitably introduces cache errors. Recent work, TaylorSeer [32], observed the continuous trajectories of the diffusion sampling procedure. By leveraging multi-step historical features via Taylor series expansion, it significantly reduced cache errors, pushing the acceleration limits of feature caching methods. However, such solutions, which involve manually constructing prediction functions based on specific prior assumptions, are inherently limited in their ability to fully capture the evolutionary trends of high-dimensional features in diffusion models. Consequently, these traditional training-free cache-based methods still exhibit noticeable loss of high-frequency and semantic details.

This paper begins with an intuitive classical phenomenon: the inherent loss of detail in traditional feature caching methods becomes more severe in step-distilled models. As shown in Figure 1(a), the sampling trajectory of diffusion models from noise to data is inherently highly continuous when using a large number of inference steps, which is precisely where traditional training-free feature caching proves effective. However, after the model undergoes step-distillation, the sampling points on the noise-data pair trajectory become sparse. Consequently, the velocity predictions generated by the step-distilled model exhibit significant discrepancies as in Figure 1(b). This makes it challenging to utilize previous features to guide and predict the model’s subsequent velocity evolution, as it can no longer be achieved through simple linear or higher-order elementary functions in traditional feature caching methods.

Therefore, we innovatively introduce *lightweight learnable neural network predictors*, rather than handcrafted prediction formulas, in such challenging prediction scenarios led by step-distillation. Through this powerful data-driven approach, the lightweight neural network predictor can effectively capture the evolutionary trends of high-dimensional features during diffusion sampling, thereby achieving more accurate predictions of these features.

Additionally, *improving the stability of step-distillation* also contributes to enhancing the final generation quality. We observed that when applied to large-scale, complex video generation models, MeanFlow cannot achieve the goal of inference in just a few steps while preserving quality. In such scenarios with high-quality requirements, the original few-step or even one-step distillation methods become overly aggressive, negatively impacting the distillation process. Therefore, *Restricted MeanFlow* is designed by limiting the sampling range of average velocities during the MeanFlow distillation process and pruning cases with excessively high compression ratios in the MeanFlow training, thereby enabling more stable distillation results.

Through dual improvements to the feature caching

and step-distillation methods, traditional training-free and training-aware approaches are made compatible, further pushing the boundaries of acceleration limits for large-scale video generation models under high-quality generation.

In summary, our main contributions are as follows:

- **Lightweight Neural Predictor for Caching:** We propose a *lightweight learnable neural predictor*, enabling further acceleration in step-distilled models with much more difficult sampling trajectories. To the best of our knowledge, the proposed *Distillation-Compatible Learnable Feature Caching* (DisCa) is the first to suggest a ‘learnable feature caching with distillation’ solution.
- **Restricted MeanFlow:** We discuss the challenges for highly compressed distillation on large-scale video models. Through pruning the highly compressed scenarios in MeanFlow training, we provide a conservative scheme, Restricted MeanFlow, for a more stable video generation.
- **State-of-the-Art Performance:** The proposed DisCa, with Restricted MeanFlow, has highly outperformed the previous methods with an almost lossless acceleration of $11.8\times$. By enabling the training-free and training-aware acceleration methods complementing each other, DisCa provides a new pathway for efficient generation.

2. Related Works

Diffusion Models (DMs) [16, 58] have increasingly demonstrated superior performance across many modalities and tasks, with particularly outstanding quality in image and video generation tasks. In recent years, the model architecture of DMs has shown a trend of evolving from the traditional U-Net structure [51] to Diffusion Transformers (DiTs) [48], primarily due to the excellent scalability of DiTs. While increasing the scale of the models enhances the quality of the generated content, this improvement comes at the cost of a substantially higher computational load for the denoising models. This issue is particularly severe in current state-of-the-art (SOTA) diffusion models [5, 6, 22, 28, 63, 65, 68, 78], which require dozens of iterative steps for the denoising process. Consequently, the demand for accelerating diffusion models has become increasingly urgent. Currently, acceleration techniques for diffusion models can mainly be categorized into *Sampling Timestep Reduction* and *Denoising Network Acceleration*.

2.1. Sampling Timestep Reduction

A straightforward and intuitive approach to acceleration is to *reduce sampling steps while preserving output quality*. DDIM [59] introduced a deterministic sampling framework that maintained generation fidelity with fewer denoising iterations. Subsequent advancements, such as the DPM-Solver series [37, 38, 77], enhanced this direction through high-order numerical ODE solvers. Flow matching [29, 34] further generalizes the diffusion process into a transformation between noise and data points, defining the evolution

path of probability distributions via a deterministic instant velocity field, improving sampling efficiency. *Step distillation methods* [45, 53, 54, 69, 70] and *Consistency models* [39, 40, 60] consolidate multiple denoising operations into a reduced number of steps or even a single sampling pass. The Shortcut model [12] cleverly combines the two by enabling the model to learn the distance between two points on the sampling trajectory. Building on this, Meanflow [14] innovatively proposes modeling the mean velocity field instead of the instantaneous velocity field, demonstrating outstanding performance in the image generation task and even showing considerable results with one-step generation. However, translating this success to video generation, which is characterized by significantly higher complexity, reveals limitations. Noticeable declines in quality are often exhibited there, even under conservative multi-step or few-step distillation scenarios. Consequently, there is a strong necessity for *a distillation scheme tailored to the demands of large models and high-quality video generation*.

2.2. Denoising Network Acceleration

Improving the single-pass computational efficiency of the denoising network is another effective direction for enhancing the computational efficiency. Current approaches can generally be categorized into techniques based on *Model Compression* and those based on *Feature Caching*.

Model Compression-based Acceleration. Model compression techniques include knowledge distillation [27], network pruning [11, 81], token reduction [2, 9, 20, 52, 73, 74], and quantization [21, 26, 57]. Recently, model grafting [4] for DiTs has also emerged as a promising direction for exploration. Although effective, these approaches are constrained by an inherent trade-off: a reduction in model size often incurs substantial degradation in output quality. Therefore, the development of compression strategies for such methods must be painstakingly precise.

Feature Caching-based Acceleration. Feature Caching has gained prominence due to its training-free nature and strong empirical performance. Initially introduced in U-Net-based diffusion models [25, 43], caching mechanisms have been adapted to address the high computational cost of Diffusion Transformers (DiTs). Recent advances include FORA [56] and Δ -DiT [7], reusing attention and MLP representations, DiTFastAttn [72] and PAB [76], reducing redundancy in self-attention across spatial, temporal, and conditional dimensions. The ToCa series [32, 33, 79, 82, 83] introduces dynamic feature updates to mitigate information loss, with TaylorSeer [32] proposing a ‘cache-then-forecast’ paradigm to significantly reduce cache loss. Additional adaptive strategies include timestep-aware caching in L2C [42], TeaCache [31], AdaCache [18], and SpeCa [33], as well as methods like FasterCache [41] with its CFG-Cache strategy. Other notable contributions are EOC’s [49]

error optimization, UniCP’s [61] unified caching-pruning framework, RAS’s [35] region-adaptive sampling, and MagCache’s [44] magnitude-aware strategy. The technique has also been extended to tasks such as image editing [67].

However, due to its training-free nature, traditional feature caching methods highly rely on tailored, handcrafted prediction strategies to enhance performance, inevitably leading to the loss of both semantic and fine-grained details. Additionally, conventional caching approaches tend to underperform on models that have undergone step distillation, primarily because the inter-step redundancy is significantly reduced after distillation, as mentioned in Figure 1.

In this work, we propose DisCa as a further improvement to the traditional feature caching and step-distillation methods, specifically MeanFlow, for its impressive performance. By pruning the aggressive compression components of MeanFlow, we significantly enhanced the stability of the distilled models. Through training, the lost details and semantic information faced by the traditional feature caching are then compensated, thereby reaching our goal of further improving computational efficiency on the distilled model.

3. Method

3.1. Preliminary

Diffusion Models. Diffusion models [16] generate structured data by iteratively denoising random noise through a series of denoising steps. Setting t as the timestep and β_t the noise variance schedule, $p_\theta(x_{t-1} | x_t)$, the conditional probability in the denoising process, can be modeled as:

$$\mathcal{N} \left(x_{t-1}; \frac{1}{\sqrt{\alpha_t}} \left(x_t - \frac{1 - \alpha_t}{\sqrt{1 - \bar{\alpha}_t}} \epsilon_\theta(x_t, t) \right), \beta_t \mathbf{I} \right), \quad (1)$$

where $\alpha_t = 1 - \beta_t$, $\bar{\alpha}_t = \prod_{i=1}^T \alpha_i$, and T denotes the total number of timesteps. Notably, ϵ_θ , a denoising network parameterized by θ , predicts the noise required for denoising from its input x_t and t . The total T iterative timesteps required for ϵ_θ during image generation represent the majority of computational expense in diffusion models. Recent studies have proved that implementing ϵ_θ as a decoder-only transformer often enhances generation quality.

Diffusion Transformer Architecture. The Diffusion Transformer (DiT) [47] employs a hierarchical structure, $\mathcal{G} = g_1 \circ g_2 \circ \dots \circ g_L$, where each block $g_l = \mathcal{F}_{\text{SA}}^l \circ \mathcal{F}_{\text{CA}}^l \circ \mathcal{F}_{\text{MLP}}^l$ comprises self-attention (SA), cross-attention (CA), and multilayer perceptron (MLP) components. The superscript $l \in \{1, 2, \dots, L\}$ denotes the layer index.

Flow Matching. Flow Matching [30] is a simple method to train Continuous Normalizing Flows (CNFs), which regresses onto a vector field that generates a target probability density path p_t . Given two marginal distributions, $q_0(x_0)$ and $q_1(x_1)$ representing data and noise, Flow Matching optimizes a regression objective to learn a CNF for transport

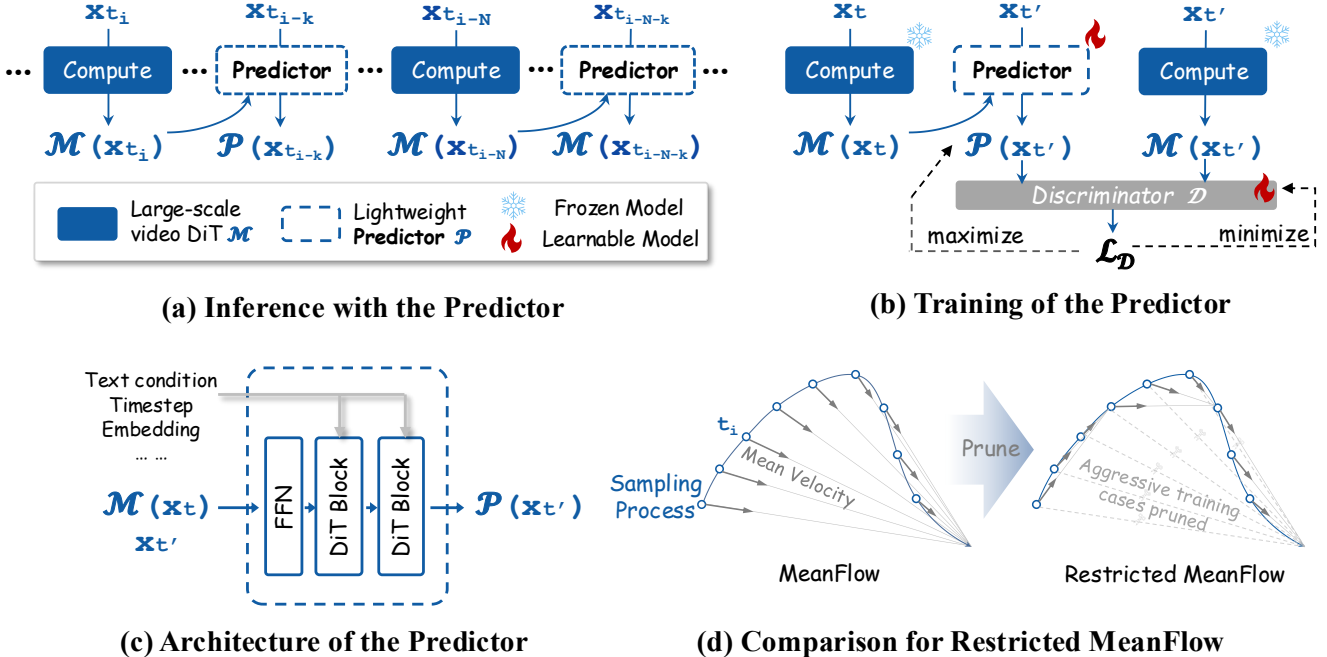


Figure 2. **An overview of Distillation-Compatible Learnable Feature Caching (DisCa).** (a) The inference procedure under the proposed Learnable Feature Caching framework. The lightweight Predictor \mathcal{P} performs multi-step fast inference after a single computation pass through the large-scale DiT \mathcal{M} . (b) **The training process of Predictor.** The cache, initialized by the DiT, is fed into the Predictor as part of the input. The outputs of the Predictor and DiT are passed to the discriminator \mathcal{D} , alternating between the objectives of maximizing and minimizing $\mathcal{L}_{\mathcal{D}}$ as part of the adversarial game. (c) **The lightweight Predictor with two DiT Blocks**, typically constitutes less than 4% of the total size of the DiT, enabling high-speed and accurate inference. (d) **The Restricted MeanFlow** is constructed primarily by pruning the components with a high compression ratio in the original MeanFlow, thereby facilitating the learning of the local mean velocity.

between them: $\mathbb{E}_{t, p_t(x)} \|v_t(x; \theta) - u_t(x)\|^2$, where $v_t(x; \theta)$ is a parametric vector field for the CNF, and $u_t(x)$ is a target vector field that generates a probability path p_t with the two marginal constraints $p_{t=0} = q_0$ and $p_{t=1} = q_1$.

Naïve Feature Caching for Diffusion Models. Recent acceleration methods employ *Naïve Feature Caching Strategies* [43, 56] in diffusion models by directly reusing computed features across adjacent timesteps. Specifically, given timesteps $\{t_i, t_{i-1}, \dots, t_{i-(N-1)}\}$, features computed at timestep t_i are cached as $\mathcal{C}(x_{t_i}^l) := \{\mathcal{F}(x_{t_i}^l)\}$. These cached features are then directly reused for subsequent steps: $\mathcal{F}(x_{t_{i-k}}^l) := \mathcal{F}(x_{t_i}^l)$, where $k \in 1, \dots, N-1$. While this approach achieves a theoretical N -fold speedup by eliminating redundant computations, it suffers from exponential error accumulation as N increases due to neglecting the temporal dynamics of features.

TaylorSeer. TaylorSeer [32] improves the ‘cache-then-reuse’ framework of naïve feature caching to ‘cache-then-forecast’. By performing a simple forecast, it achieves a significant reduction in cache error, by maintaining a cache at each layer containing the feature’s derivatives of multi-orders: $\mathcal{C}(x_t^l) := \{\mathcal{F}(x_t^l), \Delta\mathcal{F}(x_t^l), \dots, \Delta^m\mathcal{F}(x_t^l)\}$, and making predictions through a Taylor series expansion: $\mathcal{F}_{\text{pred},m}(x_{t-k}^l) = \mathcal{F}(x_t^l) + \sum_{i=1}^m \frac{\Delta^i \mathcal{F}(x_t^l)}{i! N^i} (-k)^i$.

MeanFlow. MeanFlow [14] novelly shifted the training target for few-step DMs from instant velocity to mean velocity in a physically intuitive way. The mean velocity is defined simply: $(t-r)\vec{u}(r, t, x_t) = \int_r^t \vec{v}(\tau, x_\tau) \cdot d\tau$, where \vec{u} is the mean velocity, \vec{v} is the instant velocity, t and r are the end and the start of the sampled time interval. Although feasible for discrete simulation, integration in the training/distillation process is expensive. After partial derivative transformations in [14], the optimization target is given:

$$\mathcal{L}(\theta) = \mathbb{E} \|u_\theta(x_t, r, t) - \text{sg}(u_{\text{tgt}})\|_2^2, \quad (2)$$

where $u_{\text{tgt}} = v(x_t, t) - (t-r)(v(x_t, t)\partial_x u_\theta + \partial_t u_\theta)$, u_{tgt} is the meanflow target, θ is the parameter, $u_\theta(x_t, r, t)$ is the predicted mean velocity between r and t generated by MeanFlow model with input noised latent x_t . As shown in (2), the numerical errors introduced by the derivative calculations become more severe for longer sequence generation, making it challenging for large-scale video model training.

3.2. Restricted MeanFlow

The MeanFlow, as mentioned, is designed initially aiming at the target of one-step distillation, so during the distillation, the interval \mathcal{I} between the sampled start time r and end time t , $\mathcal{I} = (t-r) \in [0, 1]$. Due to the high complexity of large-scale video generation models and the potential numerical errors mentioned, arbitrarily setting the distillation interval to $\mathcal{I} = 1$ is not feasible. To address this, we propose a Restricted MeanFlow (RMF) that only samples points within a small interval \mathcal{I} around the start time r .

tillation target to ‘one-step’ distillation can be too hard to compress for the aimed large-scale video DiTs. On the contrary, *the highly compressed part of MeanFlow significantly increases the difficulty of training, leading to catastrophic distortions in the generated results.*

Therefore, to achieve high-quality and stable generation results, a conservative sampling strategy is necessary. In cases where the goal is no longer one-step distillation but instead prioritizing quality, the larger-value portions of \mathcal{I} , corresponding to the overly aggressive parts in MeanFlow distillation, can be pruned directly. As a local and more stable solution, the Restricted MeanFlow is introduced, building up on MeanFlow with mean velocity interval \mathcal{I} sampled:

$$\mathcal{I} = (t - r) \in [0, \mathcal{R}], \quad (3)$$

where the restrict factor $\mathcal{R} \in (0, 1)$.

3.3. Learnable Feature Caching

Based on the ‘cache-then-forecast’ framework, we introduce a lightweight neural predictor to capture the high-dimensional features in DMs, therefore achieving precise predictions with the strong power of a data-driven method.

Inference Process. As mentioned in Figure 2, Cached Feature \mathcal{C} is firstly initialized, or refreshed (if this is not the first step), in a full inference step with DM:

$$\mathcal{C}(x_{t_i}) = u(x_{t_i}, r_i, t_i) = \mathcal{M}_{\theta_M}(x_{t_i}, r_i, t_i, c_{t_i}), \quad (4)$$

where \mathcal{M} denotes the large-scale DM, with the parameter θ_M , and conditional information vector c .

At the coming $N - 1$ steps, the lightweight neural Predictor is introduced, rather than full computation:

$$u(x_{t'}, r', t') = \mathcal{P}_{\theta_p}(\mathcal{C}, x_{t'}, r', t', c_{t'}), \quad (5)$$

where \mathcal{P} and \mathcal{C} denote the Predictor and cache respectively, with the corresponding paired timesteps in cached steps $(t', r') \in \{(t_{i-1}, r_{i-1}), \dots, (t_{i-(N-1)}, r_{i-(N-1)})\}$ ¹.

Predictor Training To enable the lightweight Predictor \mathcal{P} to sufficiently learn the feature evolution trend of the large model \mathcal{M} during the sampling process, we innovatively designed a cache-based predictor training scheme.

Firstly, the large-scale DM \mathcal{M} performs one sampling step, obtaining the cache \mathcal{C} as shown in (4). $\mathcal{C}(x_t) = \mathcal{M}_{\theta_M}(x_t, r, t, c_t)$, where the x_t is sampled from the noise-data interpolation: $x_t = tx_1 + (1 - t)x_0$ and (t, r) are the sampled paired timesteps under the restriction (3).

With the cache \mathcal{C} passed to the learnable lightweight Predictor, the Predictor then makes its computation as (5): $\mathcal{P}_{\theta_p}(\mathcal{C}, x_{t'}, r', t', c_{t'})$, where $(t', r') = (t - \Delta, r - \Delta)$, Δ is a sampled small timestep bias, representing the distance between the full computation step above and the current cache step. The large-scale DM replicates the predictor sampling process, providing a ground-truth $\mathcal{M}_{\theta_M}(x_{t'}, r', t', c_{t'})$.

¹For restricted MeanFlow sampling, it is obvious that the average velocity predicted by two adjacent steps should be end-to-end (or contiguous), leading to $r_j = t_{j-1}$ for all sampled (t, r) timestep pairs.

In summary, the optimization target can be written as:

$$\mathcal{L}(\theta_p) = \mathbb{E} \|\mathcal{M}_{\theta_M}(x_{t'}, r', t') - \mathcal{P}_{\theta_p}(\mathcal{C}, x_{t'}, r', t')\|_2^2, \quad (6)$$

where the cache $\mathcal{C} = \mathcal{M}_{\theta_M}(x_t, r, t, c_t)$, and condition vectors c_t and $c_{t'}$ are omitted for simplicity.

Generative Adversarial Training. To further enhance the prediction performance of the lightweight Predictor and mitigate semantic structure loss and blurriness commonly observed in traditional feature caching, a Generative Adversarial Training scheme, as in [55], is introduced.

Specifically, we employ a Multi-Scale Discriminator based on *Spectral Normalization (SN) and Hinge Loss*. This adversarial setup forces the Predictor to not only minimize error in the pixel space (as with MSE) but also to generate samples rich in high-frequency details and possessing high visual fidelity within the perceptual feature space.

In summary, the final optimization targets with Generative Adversarial loss are as follows:

$$\begin{aligned} \mathcal{L}_{\mathcal{D}} = \mathbb{E} [& \max(0, 1 - \mathcal{D} \circ \mathcal{F} \circ \mathcal{M}_{\theta_M}(x_{t'}, r', t')) \\ & + \max(0, 1 + \mathcal{D} \circ \mathcal{F} \circ \mathcal{P}_{\theta_p}(\mathcal{C}, x_{t'}, r', t'))], \end{aligned} \quad (7)$$

$$\begin{aligned} \mathcal{L}_{\mathcal{P}} = \mathbb{E} [& \|\mathcal{M}_{\theta_M}(x_{t'}, r', t') - \mathcal{P}_{\theta_p}(\mathcal{C}, x_{t'}, r', t')\|_2^2 \\ & + \lambda \cdot \max(0, 1 - \mathcal{D} \circ \mathcal{F} \circ \mathcal{P}_{\theta_p}(\mathcal{C}, x_{t'}, r', t'))], \end{aligned} \quad (8)$$

where the $\mathcal{L}_{\mathcal{D}}, \mathcal{L}_{\mathcal{P}}$ are the loss functions for discriminator \mathcal{D} and predictor \mathcal{P} , respectively. Here, \mathcal{F} denotes the feature extractor used before the discriminator \mathcal{D} . To enable feature-space adversarial training, the outputs from both the large-scale DM and the lightweight Predictor are passed to \mathcal{F} to obtain their respective multi-level feature representations. Consistent with the methodology in [55], we utilize the large-scale DM (acting as a pre-trained backbone) as the feature extractor \mathcal{F} , and λ is the weight for adversarial loss.

Predictor Architecture Design. The Decoder-Only architecture of DiTs has shown its robust processing capabilities for features, which we aim to continue in the design of the Predictor. Therefore, the Predictor \mathcal{P} is designed by stacking a small number of DiT Blocks, with a size always smaller than 4% of the large-scale model \mathcal{M} .

Memory-Efficient Feature Caching. Note that there is no superscript indicating the layer index l , which means we no longer maintain the cache composed of one or multiple tensors for each layer of the DM; instead, only a single tensor is kept during the inference procedure. This primarily benefits from the powerful learning capability of the Predictor, which eliminates the need for a structurally complex cache to provide sufficiently rich information to the training-free solution, as was previously required in TaylorSeer [32]. A Memory-Efficient cache is particularly crucial for the real-world application of high-resolution and long-term video generation models, and simultaneously significantly preserves computational efficiency in distributed

Table 1. Quantitative comparison on Restricted MeanFlow for HunyuanVideo on VBench.

Method HunyuanVideo[62]	CFG Distilled	Acceleration			VBench Score (%)		
		Latency(s) ↓	Speed ↑	Full NFE ↓	Semantic↑	Quality↑	Total↑
Original: 50 steps	✗	1155.3	1.00×	50 × 2	73.5(+0.0%)	81.5(+0.0%)	79.9(+0.0%)
CFG Distilled: 50 steps	✓	581.1	1.99×	50	66.7(-9.3%)	80.6(-1.1%)	77.9(-2.5%)
MeanFlow: 20 steps	✓	232.7	4.96×	20	66.6(+0.0%)	81.8(+0.0%)	78.8(+0.0%)
Restricted MeanFlow($\mathcal{R} = 0.4$)	✓	232.5	4.97×	20	70.2(+4.5%)	82.0(+0.2%)	79.7(+1.1%)
Restricted MeanFlow($\mathcal{R} = 0.2$)	✓	232.4	4.97×	20	70.4(+5.7%)	81.8(+0.0%)	79.5(+0.9%)
MeanFlow: 10 steps	✓	119.4	9.68×	10	60.9(+0.0%)	80.6(+0.0%)	76.7(+0.0%)
Restricted MeanFlow($\mathcal{R} = 0.4$)	✓	119.2	9.69×	10	67.6(+11.0%)	81.3(+0.9%)	78.6(+2.5%)
Restricted MeanFlow($\mathcal{R} = 0.2$)	✓	119.3	9.68×	10	68.2(+12.0%)	81.3(+0.9%)	78.7(+2.9%)

parallel environments. We will discuss this further in the following Experiments section and the Appendix.

4. Experiments

4.1. Experiment Settings

Model Configuration The experiments are conducted on HunyuanVideo [22], a state-of-the-art large-scale video DiT model. Using a checkpoint pre-trained at 540p resolution as the base, distillation and training are carried out on H20. Videos of 704×704 resolution, 129 frames, and 5 seconds in duration are generated for evaluation. In video generation scenarios involving such high resolution and long time duration, the VRAM pressure becomes crucial. Therefore, a sequence parallel size of 4 is applied.

Metrics and Evaluation For the generated videos, we use VBench [17] for evaluation. VBench comprises 16 sub-dimensions that assess video generation quality from multiple aspects. Among these, 9 aspects constitute the Semantic Score, while the others form the Quality Score. These scores are weighted to produce the Total Score. Given that the Semantic score is more sensitive to distortions and controllability in the generated results, we have selected it as the primary metric, while the others are supplementary references. More information is available in the Appendix.

Distillation and Training Configurations Starting from the initial HunyuanVideo with Classifier Free Guidance (CFG), we first perform CFG distillation with a learning rate of 10^{-5} to enable the model to directly obtain the result that previously required separate inference with and without CFG in a single forward pass. Subsequently, Restricted MeanFlow distillation is applied sequentially with the same learning rate to complete the step distillation process. Finally, a lightweight predictor is trained with a Generative-Adversarial strategy on the distilled model, with learning rates $10^{-4}, 10^{-2}$ for predictor and discriminator, respectively and a weight of adversarial loss for predictor $\lambda = 1.0$ to yield DisCa. More settings are detailed in the Appendix.

4.2. Restricted MeanFlow

Quantitative Study As shown in Table 1, results on both 20 steps and 10 steps demonstrate that the proposed Restricted

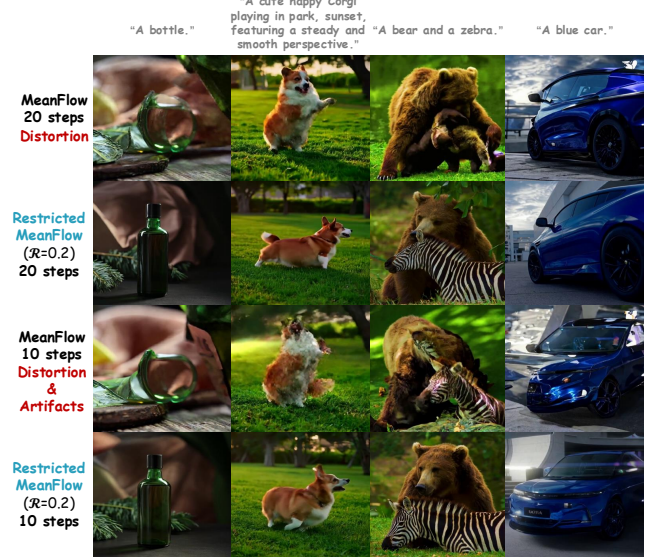


Figure 3. Qualitative Comparison for MeanFlow and the proposed Restrict MeanFlow. In the video generation scenarios for both 20 steps and 10 steps, the MeanFlow method exhibits noticeable distortion and artifacts. In contrast, the Restricted MeanFlow maintains high quality, as indicated by the metrics in Table 1.

MeanFlow significantly outperforms the original one-step-aimed MeanFlow [14], even surpassing the 50-step model trained with CFG distillation. Taking the $\mathcal{R} = 0.2$ case as an example, the proposed Restricted MeanFlow exhibits a substantial advantage in the semantic score. For the 20-step generation, it surpasses the original MeanFlow by 5.4%, and for the more aggressive 10-step generation, this lead increases to a remarkable 12.0%. It also shows superior performance in the quality score. Specifically, the massive success in the semantic score [17] indicates that the proposed Restricted MeanFlow achieves a significant improvement in terms of controllable generation and mitigating artifacts/distortions compared to the original MeanFlow.

Qualitative Study As shown in Figure 3, the proposed Restricted MeanFlow has made significant improvements under accelerated inference at both 20 steps and 10 steps. Taking the 20-step example, in the “A bottle.” and “A bear and a zebra.” cases, MeanFlow exhibits clear issues of mal-

Table 2. Quantitative comparison on different acceleration methods for HunyuanVideo on VBench.

Method	CFG Distilled	Efficiency			VBench Score (%)		
		Latency(s) \downarrow	Speed \uparrow	Peak VRAM \downarrow	Semantic \uparrow	Quality \uparrow	Total \uparrow
Original: 50 steps	\times	1155.3	1.00 \times	99.23GB	73.5(+0.0%)	81.5(+0.0%)	79.9(+0.0%)
CFG Distilled: 50 steps	\checkmark	581.1	1.99 \times	97.21GB	66.7(-9.3%)	80.6(-1.1%)	77.9(-2.5%)
Original: 10 steps	\times	234.7	4.92 \times	99.23GB	57.6(-21.6%)	75.8(-7.0%)	72.2(-9.6%)
CFG Distilled: 20 steps	\checkmark	234.4	4.93 \times	97.21GB	64.1(-12.8%)	79.6(-2.3%)	76.5(-4.3%)
Δ -DiT($N = 5$) [7]	\checkmark	306.7	3.77 \times	97.68GB	60.0(-18.4%)	76.7(-5.9%)	73.3(-8.3%)
PAB($N = 5$) [76]	\checkmark	216.5	5.34 \times	121.3GB	53.4(-27.3%)	73.1(-10.3%)	69.2(-13.4%)
TeaCache($l = 0.15$) [31]	\checkmark	237.6	5.00 \times	97.70GB	65.5(-10.9%)	80.3(-1.5%)	77.4(-3.1%)
FORA($N = 3$) [56]	\checkmark	265.7	4.35 \times	124.6GB	63.9(-13.1%)	79.7(-2.2%)	76.6(-4.1%)
TaylorSeer($N = 3, O = 1$) [32]	\checkmark	268.3	4.31 \times	130.7GB	65.2(-11.3%)	80.6(-1.1%)	77.5(-3.0%)
MeanFlow: 20 steps [14]	\checkmark	232.7	4.96 \times	97.21GB	66.6(-9.4%)	81.8(+0.4%)	78.8(-1.4%)
Restricted MeanFlow: 20 steps [Ours]	\checkmark	232.4	4.97 \times	97.21GB	70.4(-4.2%)	81.8(+0.4%)	79.5(-0.5%)
DisCa($\mathcal{R} = 0.2, N = 2$) [Ours]	\checkmark	152.8	7.56 \times	97.64GB	70.8(-3.7%)	81.9(+0.5%)	79.7(-0.3%)
CFG Distilled: 10 steps	\checkmark	119.7	9.65 \times	97.21GB	59.0(-19.7%)	76.8(-4.7%)	73.2(-8.4%)
Δ -DiT($N = 8$) [7]	\checkmark	253.7	4.55 \times	97.68GB	42.7(-41.9%)	70.9(-13.0%)	65.2(-18.4%)
PAB($N = 8$) [76]	\checkmark	178.8	6.46 \times	121.3GB	56.3(-23.4%)	76.1(-6.6%)	72.1(-9.8%)
TeaCache($l = 0.4$) [31]	\checkmark	125.3	9.22 \times	97.70GB	62.1(-15.5%)	78.7(-3.4%)	75.4(-5.6%)
FORA($N = 6$) [56]	\checkmark	144.2	8.01 \times	124.6GB	57.5(-21.8%)	76.4(-6.3%)	72.6(-9.1%)
TaylorSeer($N = 6, O = 1$) [32]	\checkmark	166.0	6.96 \times	130.7GB	63.7(-13.3%)	79.9(-2.0%)	76.7(-4.0%)
Restricted MeanFlow: 9 steps [Ours]	\checkmark	108.3	10.7 \times	97.21GB	67.8(-7.8%)	81.0(-0.6%)	78.4(-1.9%)
DisCa($\mathcal{R} = 0.2, N = 3$) [Ours]	\checkmark	130.7	8.84 \times	97.64GB	70.3(-4.4%)	81.8(+0.4%)	79.5(-0.5%)
DisCa($\mathcal{R} = 0.2, N = 4$) [Ours]	\checkmark	97.7	11.8 \times	97.64GB	69.3(-5.7%)	81.1(-0.5%)	78.8(-1.4%)

formation and collapse (or severe distortion), whereas the proposed Restricted MeanFlow still maintains high-quality generation. In the more aggressive 10-step inference, the malformation issues of MeanFlow become even more severe, producing noticeable artifacts and blending issues in the “... happy Corgi...” and “A blue car.” examples. In contrast, Restricted MeanFlow continues to guarantee quality, further demonstrating that our proposed Restricted MeanFlow, by pruning the training of the aggressive, hard-to-learn portion, effectively enhances video quality.

4.3. Distillation-Compatible Learnable Cache

Quantitative Study As shown in Table 2, the proposed DisCa achieves results that significantly surpass the comparison methods in both the low acceleration ratio and high acceleration ratio regions. Taking the high-speed region (bottom row) as an example, arbitrarily reducing the total number of sampling steps to 10 steps leads to a 19.7% semantic loss, with corresponding decreases of 4.7% and 8.4% in the Quality and Total scores, respectively. Simple ‘caching-and-reuse’ schemes like Δ -DiT [7], PAB [76], and FORA [56] completely collapse under high acceleration ratio conditions, all exhibiting a semantic drop exceeding 20%, along with a total degradation exceeding 9%. TeaCache [31], due to its adaptive caching design, manages to preserve performance to some extent but still suffers from a semantic score decrease of up to 15.5%. TaylorSeer [32], leveraging the ‘cache-then-forecast’ framework, performs the best among the various training-free acceleration schemes. However, due to the significant compression in super-high acceleration ratio scenarios, the

Table 3. Ablation study for Restrict MeanFlow, Learnbale Predictor and GAN Training in DisCa on HunyuanVideo.

Restricted MeanFlow	Learnable Predictor	GAN Training	VBench Score (%)		
			Semantic \uparrow	Quality \uparrow	Total \uparrow
\checkmark	\checkmark	\checkmark	69.3(+0.0%)	81.1(+0.0%)	78.7(+0.0%)
\times	\checkmark	\checkmark	65.2(-5.9%)	80.3(-1.0%)	77.3(-1.8%)
\checkmark	\times	—	67.3(-2.9%)	80.5(-0.7%)	77.9(-1.0%)
\checkmark	\checkmark	\times	68.5(-1.2%)	81.0(-0.1%)	78.5(-0.3%)

training-free method can no longer utilize high-dimensional feature information, resulting in a semantic loss of up to 13.3% and a total score drop of 4%. The proposed DisCa, conversely, not only outperforms Restricted MeanFlow at 4.97 \times acceleration while operating at a higher 7.56 \times acceleration, but also maintains near-lossless performance even at 8.84 \times speed. Even under a super high acceleration ratio of up to 11.8 \times , it still guarantees high-quality generation, losing only 5.7% in semantic score and 0.5% in quality, with an overall total drop of only 1.4%. This performance even shows a clear improvement compared to the 50-step CFG distilled model, further demonstrating the strong capability of learnable caching with stable distillation.

Note that DisCa is also memory efficient compared to suboptimal caching methods. This is particularly crucial in the discussed real-world scenario of generating high-resolution, long-duration videos. Even with a sequence-parallel size of 4, methods like TaylorSeer and FORA still require over 120 GB of VRAM. Furthermore, ToCa’s inability to support the Efficient Attention framework leads to excessively high VRAM consumption for long sequences. This evidence further proves that DisCa is a more suitable acceleration scheme for practical applications.

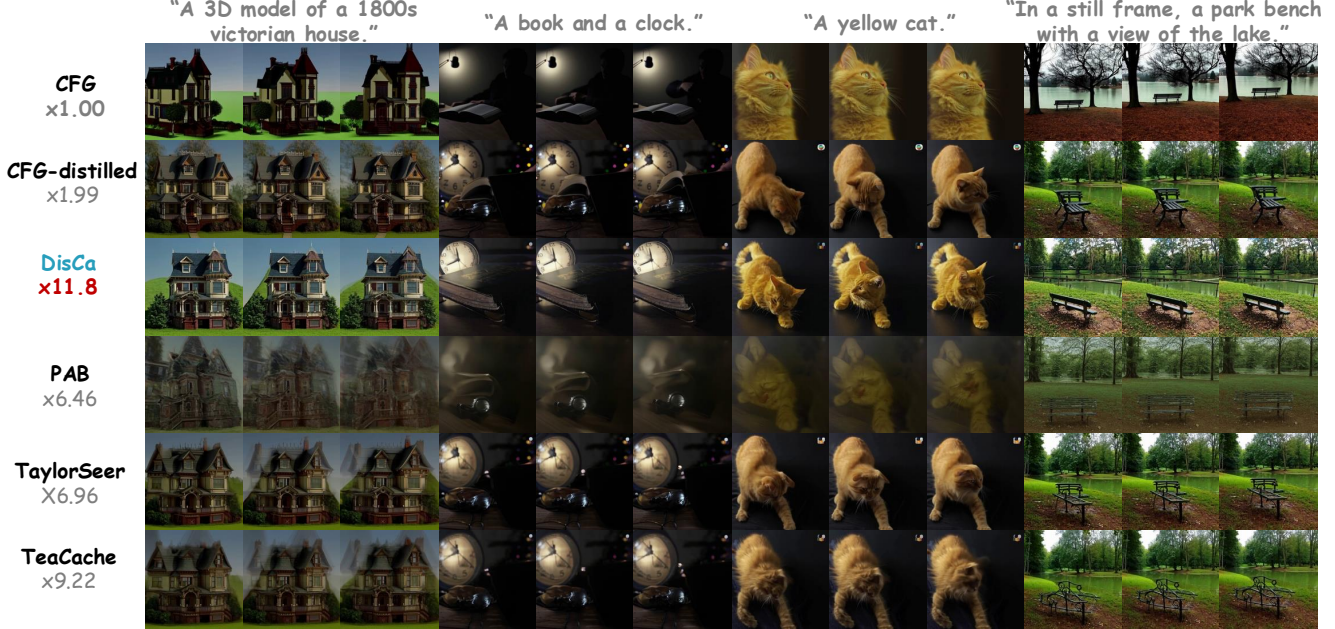


Figure 4. Visualization of acceleration methods on HunyuanVideo. In the discussed high acceleration ratio scenarios, previous methods exhibit severe degradation, such as malformation and blurring, while **DisCa** successfully maintains high quality with a $11.8\times$ acceleration.

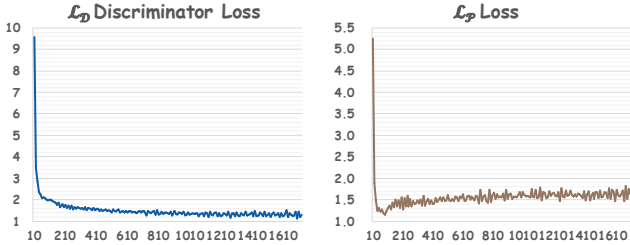


Figure 5. **Loss curve during the Generative-Adversarial training process.** The discriminator \mathcal{D} and predictor \mathcal{P} exhibit a stable adversarial dynamic, enhancing the generating capability.

Qualitative Study Figure 4 demonstrates the inference performance of various acceleration methods on HunyuanVideo. Clearly, the proposed DisCa surpasses previous acceleration methods by an overwhelming margin.

Specifically, PAB [76] exhibits noticeable blurring and artifacts across almost all cases. TaylorSeer [32] and TeaCache [31], meanwhile, display malformation and distortion in the “... victorian house.” “... the lake.” and “A book and a clock.” examples, with clear detail degradation also evident in the “A yellow cat.” case. In contrast, the proposed DisCa not only achieves an acceleration that far exceeds all comparison methods but also retains rich and diverse details while presenting clear and explicit structural information.

4.4. Ablation Study

We conducted a series of experiments to perform an ablation study on various aspects of the proposed Distillation-Compatible Learnable Feature Caching scheme, further supporting our claims. As shown in Table 3, training the cache scheme on the original MeanFlow rather than the Restricted MeanFlow leads to the most pronounced degra-

tion, resulting in a 5.9% semantic score drop. This corresponds to a *completely unacceptable malformation* in the generated output, a 1.0% decrease in the Quality score, and a 1.8% drop in the total score. This result demonstrates that pruning the overly aggressive portion during distillation is crucial for the video generation task. When accelerating the distilled model using simple training-free caching, we observed a 2.9% drop in semantic score and a 0.7% drop in quality score, *incuring unacceptable losses in both semantic fidelity and quality*. Furthermore, without employing GAN Training, the model’s semantic capability also shows a notable decline, with the semantic score decreasing by 1.2%, further demonstrating the importance of generative adversarial training for the predictor’s semantic ability.

Figure 5 displays the training losses $\mathcal{L}_{\mathcal{D}}$ and $\mathcal{L}_{\mathcal{P}}$, for the discriminator and predictor, respectively, during the GAN training process. Both losses first experience a rapid descent during the initial training phase, and subsequently engage in a stable, long-term adversarial dynamic to improve quality.

5. Conclusion

Traditional Feature Caching methods typically rely on direct reuse or simple interpolation, resulting in significant quality degradation under high compression scenarios. Motivated by the fact that the feature evolution of the diffusion model involves rich, high-dimensional information, DisCa firstly proposes overcoming this dilemma by introducing a lightweight, learnable neural predictor to fully utilize the high-dimensional information. We then apply this innovation with our proposed Restricted MeanFlow scheme, which is designed for the stable compression of large-scale

video models, successfully increasing the acceleration ratio to $11.8\times$ with high generation quality, offering a novel acceleration solution distinct from conventional wisdom.

References

- [1] Andreas Blattmann, Tim Dockhorn, Sumith Kulal, Daniel Mendelevitch, Maciej Kilian, Dominik Lorenz, Yam Levi, Zion English, Vikram Voeleti, Adam Letts, et al. Stable video diffusion: Scaling latent video diffusion models to large datasets. *arXiv preprint arXiv:2311.15127*, 2023. [1](#)
- [2] Daniel Bolya and Judy Hoffman. Token merging for fast stable diffusion. In *Proceedings of the IEEE/CVF conference on computer vision and pattern recognition*, pages 4599–4603, 2023. [3](#)
- [3] Tim Brooks, Bill Peebles, Connor Holmes, Will DePue, Yufei Guo, Li Jing, David Schnurr, Joe Taylor, Troy Luhman, Eric Luhman, Clarence Ng, Ricky Wang, and Aditya Ramesh. Video generation models as world simulators. 2024. [1](#)
- [4] Keshigeyan Chandrasegaran, Michael Poli, Daniel Y. Fu, Dongjun Kim, Lea M. Hadzic, Manling Li, Agrim Gupta, Stefano Massaroli, Azalia Mirhoseini, Juan Carlos Niebles, Stefano Ermon, and Fei-Fei Li. Exploring diffusion transformer designs via grafting. *ArXiv*, abs/2506.05340, 2025. [3](#)
- [5] Junsong Chen, Chongjian Ge, Enze Xie, Yue Wu, Lewei Yao, Xiaozhe Ren, Zhongdao Wang, Ping Luo, Huchuan Lu, and Zhenguo Li. Pixart- α : Weak-to-strong training of diffusion transformer for 4k text-to-image generation, 2024. [2](#)
- [6] Junsong Chen, Jincheng Yu, Chongjian Ge, Lewei Yao, Enze Xie, Yue Wu, Zhongdao Wang, James Kwok, Ping Luo, Huchuan Lu, and Zhenguo Li. Pixart- α : Fast training of diffusion transformer for photorealistic text-to-image synthesis. In *International Conference on Learning Representations*, 2024. [2](#)
- [7] Pengtao Chen, Mingzhu Shen, Peng Ye, Jianjian Cao, Chongjun Tu, Christos-Savvas Bouganis, Yiren Zhao, and Tao Chen. δ -dit: A training-free acceleration method tailored for diffusion transformers. *arXiv preprint arXiv:2406.01125*, 2024. [3, 7, 2](#)
- [8] Yushen Chen, Zhikang Niu, Ziyang Ma, Keqi Deng, Chun-hui Wang, Jian Zhao, Kai Yu, and Xie Chen. F5-tts: A fairytaler that fakes fluent and faithful speech with flow matching. *arXiv preprint arXiv:2410.06885*, 2024. [1](#)
- [9] Xinle Cheng, Zhuoming Chen, and Zhihao Jia. Cat pruning: Cluster-aware token pruning for text-to-image diffusion models, 2025. [3](#)
- [10] Sefik Emre Eskimez, Xiaofei Wang, Manthan Thakker, Can-run Li, Chung-Hsien Tsai, Zhen Xiao, Hemin Yang, Zirun Zhu, Min Tang, Xu Tan, Yanqing Liu, Sheng Zhao, and Naoyuki Kanda. E2 tts: Embarrassingly easy fully non-autoregressive zero-shot tts. *2024 IEEE Spoken Language Technology Workshop (SLT)*, pages 682–689, 2024. [1](#)
- [11] Gongfan Fang, Xinyin Ma, and Xinchao Wang. Structural pruning for diffusion models. *arXiv preprint arXiv:2305.10924*, 2023. [3](#)
- [12] Kevin Frans, Danijar Hafner, Sergey Levine, and Pieter Abbeel. One step diffusion via shortcut models. *ArXiv*, abs/2410.12557, 2024. [1, 3](#)
- [13] Yiyang Geng, Huai Xu, Yanyong Zhang, and Fuxin Zhang. Omnicache: A unified cache for efficient query handling in lsm-tree based key-value stores. *2024 IEEE International Conference on High Performance Computing and Communications (HPCC)*, pages 353–360, 2024. [1](#)
- [14] Zhengyang Geng, Mingyang Deng, Xingjian Bai, J. Zico Kolter, and Kaiming He. Mean flows for one-step generative modeling. *ArXiv*, abs/2505.13447, 2025. [1, 3, 4, 6, 7, 2](#)
- [15] Jonathan Ho, Ajay Jain, and Pieter Abbeel. Denoising Diffusion Probabilistic Models, 2020. *arXiv:2006.11239* [cs]. [1](#)
- [16] Jonathan Ho, Ajay Jain, and Pieter Abbeel. Denoising diffusion probabilistic models. *Advances in neural information processing systems*, 33:6840–6851, 2020. [1, 2, 3](#)
- [17] Ziqi Huang, Yinan He, Jiashuo Yu, Fan Zhang, Chenyang Si, Yuming Jiang, Yuanhan Zhang, Tianxing Wu, Qingyang Jin, Nattapol Chanpaisit, Yaohui Wang, Xinyuan Chen, Limin Wang, Dahua Lin, Yu Qiao, and Ziwei Liu. Vbench: Comprehensive Benchmark Suite for Video Generative Models, 2023. *arXiv:2311.17982* [cs]. [6, 1](#)
- [18] Kumara Kahatapitiya, Haozhe Liu, Sen He, Ding Liu, Menglin Jia, Michael S. Ryoo, and Tian Xie. Adaptive caching for faster video generation with diffusion transformers. *ArXiv*, abs/2411.02397, 2024. [3](#)
- [19] Kumara Kahatapitiya, Haozhe Liu, Sen He, Ding Liu, Menglin Jia, Chenyang Zhang, Michael S. Ryoo, and Tian Xie. Adaptive Caching for Faster Video Generation with Diffusion Transformers, 2024. [1](#)
- [20] Minchul Kim, Shangqian Gao, Yen-Chang Hsu, Yilin Shen, and Hongxia Jin. Token fusion: Bridging the gap between token pruning and token merging. In *Proceedings of the IEEE/CVF Winter Conference on Applications of Computer Vision*, pages 1383–1392, 2024. [3](#)
- [21] Sungbin Kim, Hyunwuk Lee, Wonho Cho, Mincheol Park, and Won Woo Ro. Ditto: Accelerating diffusion model via temporal value similarity. In *Proceedings of the 2025 IEEE International Symposium on High-Performance Computer Architecture (HPCA)*. IEEE, 2025. [3](#)
- [22] Weijie Kong, Qi Tian, Zijian Zhang, Rox Min, Zuozhuo Dai, Jin Zhou, Jiangfeng Xiong, Xin Li, Bo Wu, Jianwei Zhang, et al. Hunyuanyvideo: A systematic framework for large video generative models. *arXiv preprint arXiv:2412.03603*, 2024. [1, 2, 6](#)
- [23] PKU-Yuan Lab and Tuzhan AI etc. Open-sora-plan, 2024. [1](#)
- [24] Black Forest Labs. Flux. <https://github.com/black-forest-labs/flux>, 2024. [1](#)
- [25] Senmao Li, Taihang Hu, Fahad Shahbaz Khan, Linxuan Li, Shiqi Yang, Yaxing Wang, Ming-Ming Cheng, and Jian Yang. Faster diffusion: Rethinking the role of unet encoder in diffusion models. *arXiv preprint arXiv:2312.09608*, 2023. [1, 3](#)
- [26] Xiuyu Li, Yijiang Liu, Long Lian, Huanrui Yang, Zhen Dong, Daniel Kang, Shanghang Zhang, and Kurt Keutzer. Q-diffusion: Quantizing diffusion models. In *2023 IEEE/CVF*

- International Conference on Computer Vision (ICCV)*, pages 17489–17499, 2023. 3
- [27] Yanyu Li, Huan Wang, Qing Jin, Ju Hu, Pavlo Chemerys, Yun Fu, Yanzhi Wang, Sergey Tulyakov, and Jian Ren. Snapfusion: Text-to-image diffusion model on mobile devices within two seconds. *Advances in Neural Information Processing Systems*, 36, 2024. 3
- [28] Zhimin Li, Jianwei Zhang, and and others Lin. Hunyuan-DiT: A powerful multi-resolution diffusion transformer with fine-grained chinese understanding. 1, 2
- [29] Yaron Lipman, Ricky T. Q. Chen, Heli Ben-Hamu, Maximilian Nickel, and Matt Le. Flow matching for generative modeling. *ArXiv*, abs/2210.02747, 2022. 2
- [30] Yaron Lipman, Ricky T. Q. Chen, Heli Ben-Hamu, Maximilian Nickel, and Matt Le. Flow Matching for Generative Modeling, 2023. 3
- [31] Feng Liu, Shiwei Zhang, Xiaofeng Wang, Yujie Wei, Haonan Qiu, Yuzhong Zhao, Yingya Zhang, Qixiang Ye, and Fang Wan. Timestep embedding tells: It's time to cache for video diffusion model, 2024. 1, 3, 7, 8, 2
- [32] Jiacheng Liu, Chang Zou, Yuanhuiyi Lyu, Junjie Chen, and ICCV 2025 Zhang, Linfeng, booktitle = International Conference on Computer Vision. From reusing to forecasting: Accelerating diffusion models with taylorseers. 2025. 2, 3, 4, 5, 7, 8
- [33] Jiacheng Liu, Chang Zou, Yuanhuiyi Lyu, Kaixin Li, Shaobo Wang, and Linfeng Zhang. Specia: Accelerating diffusion transformers with speculative feature caching. In *Proceedings of the 33rd ACM International Conference on Multimedia (MM '25)*, page to appear, Dublin, Ireland, 2025. ACM. 3
- [34] Xingchao Liu, Chengyue Gong, et al. Flow straight and fast: Learning to generate and transfer data with rectified flow. In *The Eleventh International Conference on Learning Representations*, 2023. 2
- [35] Ziming Liu, Yifan Yang, Chengruidong Zhang, Yiqi Zhang, Lili Qiu, Yang You, and Yuqing Yang. Region-adaptive sampling for diffusion transformers, 2025. 3
- [36] Cheng Lu and Yang Song. Simplifying, stabilizing and scaling continuous-time consistency models. In *International Conference on Learning Representations*, 2025. 1
- [37] Cheng Lu, Yuhao Zhou, Fan Bao, Jianfei Chen, Chongxuan Li, and Jun Zhu. Dpm-solver: A fast ode solver for diffusion probabilistic model sampling in around 10 steps. *Advances in Neural Information Processing Systems*, 35:5775–5787, 2022. 2
- [38] Cheng Lu, Yuhao Zhou, Fan Bao, Jianfei Chen, Chongxuan Li, and Jun Zhu. Dpm-solver++: Fast solver for guided sampling of diffusion probabilistic models. *arXiv preprint arXiv:2211.01095*, 2022. 2
- [39] Simian Luo, Yiqin Tan, Longbo Huang, Jian Li, and Hang Zhao. Latent consistency models: Synthesizing high-resolution images with few-step inference. *ArXiv*, abs/2310.04378, 2023. 3
- [40] Zhengyao Lv, Chenyang Si, Tianlin Pan, Zhaoxi Chen, Kwan-Yee K. Wong, Yu Qiao, and Ziwei Liu. Dcm: Dual-expert consistency model for efficient and high-quality video generation. *ArXiv*, abs/2506.03123, 2025. 3
- [41] Zhengyao Lv, Chenyang Si, Junhao Song, Zhenyu Yang, Yu Qiao, Ziwei Liu, and Kwan-Yee K. Wong. Fastercache: Training-free video diffusion model acceleration with high quality. In *Proceedings of the 13th International Conference on Learning Representations (ICLR 2025)*, 2025. 1, 3
- [42] Xinyin Ma, Gongfan Fang, Michael Bi Mi, and Xinchao Wang. Learning-to-cache: Accelerating diffusion transformer via layer caching. *arXiv preprint arXiv:2406.01733*, 2024. 1, 3
- [43] Xinyin Ma, Gongfan Fang, and Xinchao Wang. Deepcache: Accelerating diffusion models for free. In *Proceedings of the IEEE/CVF Conference on Computer Vision and Pattern Recognition*, pages 15762–15772, 2024. 1, 3, 4
- [44] Zehong Ma, Longhui Wei, Feng Wang, Shiliang Zhang, and Qi Tian. Magcache: Fast video generation with magnitude-aware cache. *ArXiv*, abs/2506.09045, 2025. 3
- [45] Chenlin Meng, Ruiqi Gao, Diederik P Kingma, Stefano Ermon, Jonathan Ho, and Tim Salimans. On distillation of guided diffusion models. In *NeurIPS 2022 Workshop on Score-Based Methods*, 2022. 3
- [46] Shen Nie, Fengqi Zhu, Zebin You, Xiaolu Zhang, Jingyang Ou, Jun Hu, Jun Zhou, Yankai Lin, Ji-Rong Wen, and Chongxuan Li. Large language diffusion models. *ArXiv*, abs/2502.09992, 2025. 1
- [47] William Peebles and Saining Xie. Scalable Diffusion Models with Transformers, 2023. arXiv:2212.09748 [cs]. 3
- [48] William Peebles and Saining Xie. Scalable diffusion models with transformers. In *Proceedings of the IEEE/CVF International Conference on Computer Vision*, pages 4195–4205, 2023. 2
- [49] Junxiang Qiu, Shuo Wang, Jinda Lu, Lin Liu, Houcheng Jiang, and Yanbin Hao. Accelerating diffusion transformer via error-optimized cache, 2025. 3
- [50] Robin Rombach, Andreas Blattmann, Dominik Lorenz, Patrick Esser, and Björn Ommer. High-resolution image synthesis with latent diffusion models. In *Proceedings of the IEEE/CVF conference on computer vision and pattern recognition*, pages 10684–10695, 2022. 1
- [51] Olaf Ronneberger, Philipp Fischer, and Thomas Brox. U-net: Convolutional networks for biomedical image segmentation. In *Medical image computing and computer-assisted intervention–MICCAI 2015: 18th international conference, Munich, Germany, October 5–9, 2015, proceedings, part III 18*, pages 234–241. Springer, 2015. 2
- [52] Omid Saghatelian, Atiye Gh. Moghadam, and Ahmad Nickabadi. Cached adaptive token merging: Dynamic token reduction and redundant computation elimination in diffusion model, 2025. 3
- [53] Tim Salimans and Jonathan Ho. Progressive distillation for fast sampling of diffusion models. *arXiv preprint arXiv:2202.00512*, 2022. 3
- [54] Tim Salimans, Thomas Mensink, Jonathan Heek, and Emiel Hoogeboom. Multistep distillation of diffusion models via moment matching. *ArXiv*, abs/2406.04103, 2024. 3
- [55] Axel Sauer, Dominik Lorenz, A. Blattmann, and Robin Rombach. Adversarial diffusion distillation. In *European Conference on Computer Vision*, 2023. 5

- [56] Pratheba Selvaraju, Tianyu Ding, Tianyi Chen, Ilya Zharkov, and Luming Liang. Fora: Fast-forward caching in diffusion transformer acceleration. *arXiv preprint arXiv:2407.01425*, 2024. 3, 4, 7, 2
- [57] Yuzhang Shang, Zhihang Yuan, Bin Xie, Bingzhe Wu, and Yan Yan. Post-training quantization on diffusion models. In *Proceedings of the IEEE/CVF conference on computer vision and pattern recognition*, pages 1972–1981, 2023. 3
- [58] Jascha Sohl-Dickstein, Eric Weiss, Niru Maheswaranathan, and Surya Ganguli. Deep unsupervised learning using nonequilibrium thermodynamics. In *International conference on machine learning*, pages 2256–2265. PMLR, 2015. 1, 2
- [59] Jiaming Song, Chenlin Meng, and Stefano Ermon. Denoising diffusion implicit models. In *International Conference on Learning Representations*, 2021. 2
- [60] Yang Song, Prafulla Dhariwal, Mark Chen, and Ilya Sutskever. Consistency models. In *International Conference on Machine Learning*, pages 32211–32252. PMLR, 2023. 3
- [61] Wenzhang Sun, Qirui Hou, Donglin Di, Jiahui Yang, Yongjia Ma, and Jianxun Cui. Unicp: A unified caching and pruning framework for efficient video generation, 2025. 3
- [62] Xingwu Sun, Yanfeng Chen, Huang, et al. Hunyuan-large: An open-source MoE model with 52 billion activated parameters by tencent. 6, 7, 2
- [63] Tencent Hunyuan Team. Hunyuanimage 2.1: An efficient diffusion model for high-resolution (2k) text-to-image generation. <https://github.com/Tencent-Hunyuan/HunyuanImage-2.1>, 2025. 1, 2
- [64] Tencent Hunyuan Foundation Model Team. Hunyuanvideo 1.5 technical report, 2025. 1
- [65] Team Wan, Ang Wang, Baole Ai, Bin Wen, Chaojie Mao, Chen-Wei Xie, Di Chen, Fei Yu, Haiming Zhao, Jianxiao Yang, Jianyuan Zeng, Jiayu Wang, Jingfeng Zhang, Jingen Zhou, Jinkai Wang, Jixuan Chen, Kai Zhu, Kang Zhao, Keyu Yan, Lianghua Huang, Mengyang Feng, Ningyi Zhang, Pandeng Li, Pingyu Wu, Ruihang Chu, Ruili Feng, Shiwei Zhang, Siyang Sun, Tao Fang, Tianxing Wang, Tianyi Gui, Tingyu Weng, Tong Shen, Wei Lin, Wei Wang, Wei Wang, Wenmeng Zhou, Wente Wang, Wenting Shen, Wenyuan Yu, Xianzhong Shi, Xiaoming Huang, Xin Xu, Yan Kou, Yangyu Lv, Yifei Li, Yijing Liu, Yiming Wang, Yingya Zhang, Yitong Huang, Yong Li, You Wu, Yu Liu, Yulin Pan, Yun Zheng, Yuntao Hong, Yupeng Shi, Yutong Feng, Zeyin Jiang, Zhen Han, Zhi-Fan Wu, and Ziyu Liu. Wan: Open and advanced large-scale video generative models. 1, 2
- [66] Chenfei Wu, Jiahao Li, Jingren Zhou, Junyang Lin, Kaiyuan Gao, Kun Yan, Shengming Yin, Shuai Bai, Xiao Xu, Yilei Chen, Yuxiang Chen, Zecheng Tang, Zekai Zhang, Zhengyi Wang, An Yang, Bowen Yu, Chen Cheng, Dayiheng Liu, Deqing Li, Hang Zhang, Hao Meng, Hu Wei, Jingyuan Ni, Kai Chen, Kuan Cao, Liang Peng, Lin Qu, Minggang Wu, Peng Wang, Shuteng Yu, Tingkun Wen, Wensen Feng, Xiaoxiao Xu, Yi Wang, Yichang Zhang, Yongqiang Zhu, Yujia Wu, Yuxuan Cai, and Zenan Liu. Qwen-image technical report, 2025. 1
- [67] Zexuan Yan, Yue Ma, Chang Zou, Wenteng Chen, Qifeng Chen, and Linfeng Zhang. EEdit : Rethinking the Spatial and Temporal Redundancy for Efficient Image Editing, 2025. 3
- [68] Zhuoyi Yang, Jiayan Teng, Wendi Zheng, Ming Ding, Shiyu Huang, Jiazhen Xu, Yuanming Yang, Wenyi Hong, Xiaohan Zhang, Guanyu Feng, Da Yin, Xiaotao Gu, Yuxuan Zhang, Weihan Wang, Yean Cheng, Bin Xu, Yuxiao Dong, and Jie Tang. Cogvideox: Text-to-video diffusion models with an expert transformer. In *The Thirteenth International Conference on Learning Representations*, 2025. 1, 2
- [69] Tianwei Yin, Michael Gharbi, Richard Zhang, Eli Shechtman, Frédéric Durand, William T. Freeman, and Taesung Park. One-step diffusion with distribution matching distillation. *2024 IEEE/CVF Conference on Computer Vision and Pattern Recognition (CVPR)*, pages 6613–6623, 2023. 1, 3
- [70] Tianwei Yin, Michaël Gharbi, Richard Zhang, Eli Shechtman, Frédéric Durand, William T Freeman, and Taesung Park. One-step diffusion with distribution matching distillation. In *Proceedings of the IEEE/CVF Conference on Computer Vision and Pattern Recognition*, pages 6613–6623, 2024. 1, 3
- [71] Tianwei Yin, Qiang Zhang, Richard Zhang, William T. Freeman, Frédéric Durand, Eli Shechtman, and Xun Huang. From slow bidirectional to fast autoregressive video diffusion models. *2025 IEEE/CVF Conference on Computer Vision and Pattern Recognition (CVPR)*, pages 22963–22974, 2024. 1
- [72] Zhihang Yuan, Hanling Zhang, Lu Pu, Xuefei Ning, Linfeng Zhang, Tianchen Zhao, Shengen Yan, Guohao Dai, and Yu Wang. DiTFastattn: Attention compression for diffusion transformer models. In *The Thirty-eighth Annual Conference on Neural Information Processing Systems*, 2024. 1, 3
- [73] Evelyn Zhang, Bang Xiao, Jiayi Tang, Qianli Ma, Chang Zou, Xuefei Ning, Xuming Hu, and Linfeng Zhang. Token pruning for caching better: 9 times acceleration on stable diffusion for free, 2024. 3
- [74] Evelyn Zhang, Jiayi Tang, Xuefei Ning, and Linfeng Zhang. Training-free and hardware-friendly acceleration for diffusion models via similarity-based token pruning. In *Proceedings of the AAAI Conference on Artificial Intelligence*, 2025. 3
- [75] Haiyu Zhang, Xinyuan Chen, Yaohui Wang, Xihui Liu, Yunhong Wang, and Yu Qiao. Accvideo: Accelerating video diffusion model with synthetic dataset. *ArXiv*, abs/2503.19462, 2025. 1
- [76] Xuanlei Zhao, Xiaolong Jin, Kai Wang, and Yang You. Real-time video generation with pyramid attention broadcast. *arXiv preprint arXiv:2408.12588*, 2024. 3, 7, 8, 2
- [77] Kaiwen Zheng, Cheng Lu, Jianfei Chen, and Jun Zhu. DPM-solver-v3: Improved diffusion ODE solver with empirical model statistics. In *Thirty-seventh Conference on Neural Information Processing Systems*, 2023. 2
- [78] Zangwei Zheng, Xiangyu Peng, Tianji Yang, Chenhui Shen, Shenggui Li, Hongxin Liu, Yukun Zhou, Tianyi Li, and Yang You. Open-sora: Democratizing efficient video production for all, 2024. 2
- [79] Zhixin Zheng, Xinyu Wang, Chang Zou, Shaobo Wang, and Linfeng Zhang. Compute only 16 tokens in one timestep: Accelerating Diffusion Transformers with Cluster-Driven

- Feature Caching. In *Proceedings of the 33rd ACM International Conference on Multimedia (MM '25)*, page to appear, Dublin, Ireland, 2025. ACM. [3](#)
- [80] Fengqi Zhu, Rongzheng Wang, Shen Nie, Xiaolu Zhang, Chunwei Wu, Jun Hu, Jun Zhou, Jianfei Chen, Yankai Lin, Ji-Rong Wen, and Chongxuan Li. Llada 1.5: Variance-reduced preference optimization for large language diffusion models. *ArXiv*, abs/2505.19223, 2025. [1](#)
- [81] Haowei Zhu, Dehua Tang, Ji Liu, Mingjie Lu, Jintu Zheng, Jinzhang Peng, Dong Li, Yu Wang, Fan Jiang, Lu Tian, Spandan Tiwari, Ashish Sirasao, Jun-Hai Yong, Bin Wang, and Emad Barsoum. Dip-go: A diffusion pruner via few-step gradient optimization, 2024. [3](#)
- [82] Chang Zou, Evelyn Zhang, Runlin Guo, Haohang Xu, Conghui He, Xuming Hu, and Linfeng Zhang. Accelerating diffusion transformers with dual feature caching, 2024. [3](#)
- [83] Chang Zou, Xuyang Liu, Ting Liu, Siteng Huang, and Linfeng Zhang. Accelerating diffusion transformers with token-wise feature caching. In *Proceedings of the 13th International Conference on Learning Representations (ICLR 2025)*. ICLR, 2025. accepted to ICLR 2025. [1](#), [3](#)

DisCa: Accelerating Video Diffusion Transformers with Distillation-Compatible Learnable Feature Caching

Supplementary Material

6. Experiment details

6.1. Training and Distillation settings

Starting with the HunyuanVideo with Classifier-Free-Guidance (CFG), we first completed CFG distillation using a learning rate of $lr = 10^{-5}$. Specifically, instead of inferring the CFG and No-CFG branches separately, we utilized a small FFN to append the input CFG information to the condition vector, thereby learning the behavior under different CFG settings. During this distillation process, the CFG was randomly sampled within the range of 1.0 to 8.0.

The model, after CFG distillation, already achieves a theoretical $2\times$ speedup compared to the original. Building on this, we proceeded with MeanFlow distillation (which is the Restricted MeanFlow discussed in this paper) using a learning rate of $lr = 10^{-5}$. We conducted experiments with Restricted MeanFlow at $\mathcal{R} = 0.4$ and $\mathcal{R} = 0.2$. Given that the $\mathcal{R} = 0.2$ version exhibited fewer artifacts, it was adopted as the foundation for DisCa training.

For DisCa training, we first used MSE loss (with a learning rate of 10^{-4}) and random cache reuse intervals $\Delta = (t - t')$ sampled between 0 to $\Delta_{max} = 0.2$ for a 500-iter initialization. We then introduced the discriminator for generative-adversarial training. The learning rate for the predictor was set to 10^{-4} and the discriminator's learning rate was set to 10^{-2} , with the weight of generative-adversarial loss for predictor training $\lambda = 1.0$. Experiments confirmed that these settings ensured a stable adversarial dynamic between the two. The final results were obtained after 1000 iters of GAN training.

6.2. Discussions on VBench

VBench [17] is applied for evaluating the generated videos. VBench consists of 16 sub-dimensions that comprehensively assess video generation quality from multiple aspects. Among these, object class, multiple objects, human action, color, spatial relationship, scene, appearance style, temporal style, and overall consistency constitute the Semantic Score, measuring the model's semantic control capability. Meanwhile, subject consistency, background consistency, temporal flickering, motion smoothness, aesthetic quality, imaging quality, and dynamic degree form the Quality Score, evaluating the overall quality of the generated videos. These two scores are then weighted to produce the Total Score with a ratio of “Semantic : Quality = 1 : 4”.

Such a scoring strategy may partially reflect a model's

capabilities and the knowledge it encapsulates. However, for critical issues in real-world application scenarios, such as **malformation, blurring, and other fatal flaws**, the Quality score, despite being weighted heavily, fails to respond effectively to them. This can be observed by comparing the visuals in Figure 3 and Figure 4 with the metrics in Table 1 and Table 2: For instance, in Figure 3, the MeanFlow 10-step example exhibits obvious malformation, while the Restricted MeanFlow 10-step example is free of such issues, yet the difference in their Quality scores is only 0.9%. Besides, in Figure 4, the PAB output is completely blurred or even collapsed due to excessive acceleration, but the corresponding Quality score in Table 2 only drops by 6.3% compared to the non-accelerated model, suggesting relying on the Quality score or even the Total score as the primary metric for this paper is clearly unreasonable.

Conversely, the **Semantic score responds well to such fatal issues**, frequently showing the most dramatic decline in the aforementioned scenarios characterized by distinct distortion and quality loss. Therefore, we elect to use the Semantic score as the primary metric, with the Quality and Total scores serving only as supplementary references.

6.3. Comparison Configurations

The acceleration methods mentioned above in Table 2 can be categorized into the low-speed region (middle) and the high-speed region (lower). We briefly introduce their computational distribution configurations here:

CFG Distilled & (Restricted) MeanFlow: Simply samples with the CFG-distilled model at a specified number of steps, such as 20 and 10 steps. The acceleration ratio is $2\times$ that of the original model (at the same given step count).

Δ -DiT: For the Multi-Modal DiT (MMDiT) structure in HunyuanVideo composed of 20 Double-Stream layers and 40 Single-Stream layers, Δ -DiT skips the 40 Single-Stream layers via a residual-form cache at every cache step. After one complete computation step, it skips $(N - 1)$ subsequent steps with cache. The configurations for the low- and high-speed regions are set to $N = 5$ and $N = 8$, respectively.

PAB: In the MMDiT architecture, the traditional distinction between Spatial-Temporal Attention and Cross-Attention does not exist. Therefore, the conventional hierarchical Attention caching strategy degenerates into periodically caching and reusing all Attention outputs. Here, the configurations for the low-speed and high-speed regions are set to $N = 5$ and $N = 8$, respectively.

TeaCache: TeaCache utilizes timestep embedding informa-

Table 4. Comparison for the theoretical and actual acceleration of different methods on HunyuanVideo.

Method	CFG Distilled	Peak VRAM	Theoretical			Actual	
			FLOPs(T)↓	Speed ↑	Latency(s)↓	Latency(s)↓	Speed↑
Original: 50 steps	✗	99.23GB	394552.32	1.00×	1155.3	1155.3	1.00×
CFG Distilled: 50 steps	✓	97.21GB	197276.16	2.00×	577.7	581.1	1.99×
Original: 10 steps	✗	99.23GB	78910.46	5.00×	231.1	234.7	4.92×
CFG Distilled: 20 steps	✓	97.21GB	78910.46	5.00×	231.1	234.4	4.93×
$\Delta\text{-DiT}(N=5)$ [7]	✓	97.68GB	92068.57	4.29×	269.3	306.7	3.77×
PAB(N = 5) [76]	✓	121.3GB	64688.07	6.10×	189.4	216.5	5.34×
TeaCache($l = 0.15$) [31]	✓	97.70GB	75350.10	5.24×	220.5	237.6	4.86×
FORA($N = 3$) [56]	✓	124.6GB	78910.46	5.00×	231.1	265.7	4.35×
TaylorSeer($N = 3, O = 1$) [32]	✓	130.7GB	78910.46	5.00×	231.1	268.3	4.31×
MeanFlow: 20 steps [14]	✓	97.21GB	78910.46	5.00×	231.1	232.7	4.96×
Restricted MeanFlow: 20 steps [Ours]	✓	97.21GB	78910.46	5.00×	231.1	232.4	4.97×
DisCa($\mathcal{R} = 0.2, N = 2$) [Ours]	✓	97.64GB	52239.36	7.55×	153.0	152.8	7.56×
CFG Distilled: 10 steps	✓	97.21GB	39455.23	10.0×	115.5	119.7	9.65×
$\Delta\text{-DiT}(N=8)$ [7]	✓	97.68GB	84178.00	4.69×	246.3	253.7	4.55×
PAB($N = 8$) [76]	✓	121.3GB	58058.68	6.80×	169.9	178.8	6.46×
TeaCache($l = 0.4$) [31]	✓	97.70GB	40779.21	9.68×	119.3	125.3	9.22×
FORA($N = 6$) [56]	✓	124.6GB	35509.71	11.1×	108.3	144.2	8.01×
TaylorSeer($N = 6, O = 1$) [32]	✓	130.7GB	43400.76	9.09×	127.1	166.0	6.96×
Restricted MeanFlow: 9 steps [Ours]	✓	97.21GB	35509.71	11.1×	104.0	108.3	10.7×
DisCa($\mathcal{R} = 0.2, N = 3$) [Ours]	✓	97.64GB	44619.05	8.84×	130.7	130.7	8.84×
DisCa($\mathcal{R} = 0.2, N = 4$) [Ours]	✓	97.64GB	33188.56	11.9×	97.1	97.7	11.8×

tion to achieve dynamic adjustment of computational allocation. It skips the cache step by performing **one** final reuse at the end. Here, the error threshold ℓ is set to 0.15 for the low-speed region and 0.4 for the high-speed region.

FORA: FORA achieves acceleration by caching and reusing the neural network parts within the residual networks corresponding to Attention and MLP in each DiT Block. Here, the configurations for the low-speed and high-speed regions are set to $N = 3$ and $N = 6$, respectively.

TaylorSeer: TaylorSeer’s cache design is similar to FORA’s but introduces caching with more derivative tensors, leading to higher VRAM occupancy but noticeably improved performance. Here, we align with the 3-step warm-up strategy from the original paper’s code to protect structural information. The configurations for the low- and high-speed regions are $N = 3$ and $N = 6$, respectively.

DisCa: As introduced previously, DisCa performs further acceleration on the Restricted MeanFlow distilled 20-step model with the introduction of a lightweight learnable predictor. N represents the maximum allowed cache interval during inference. For $N = 4, 3, 2$, the inference alternates between 8,11,13 DiT inferences and corresponding 12,9,7 predictor inferences, respectively. Crucially, the inference cost of the predictor in these scenarios is almost negligible.

6.4. Acceleration with Distributed Parallel

6.4.1. VRAM analysis

As shown in Figure 6, we analyzed VRAM consumption for each method, separating it into two parts: model with

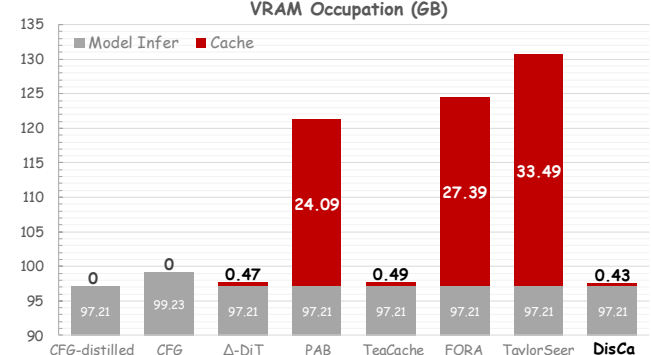


Figure 6. VRAM Occupation analysis for different acceleration methods. The VRAM consumption among different caching methods varies significantly; the proposed **DisCa** incurs only about 0.4 GB of extra VRAM overhead, which is negligible.

forward inference and cache occupancy. It can be observed that TeaCache, $\Delta\text{-DiT}$, and the proposed **DisCa** all incur negligible extra VRAM overhead. Conversely, caching schemes such as PAB, FORA, and TaylorSeer, which rely on multi-layer caching to provide richer information, generate significant VRAM overhead, increasing the demands on the operating device. Specifically, TaylorSeer, which performed optimally among previous methods, consumes an additional 33.49 GB of VRAM. In contrast, **DisCa**, while achieving higher acceleration and higher quality (as shown in Table 2), incurs only 0.43GB of additional VRAM overhead, compressing the extra VRAM cost to just 1.3%.

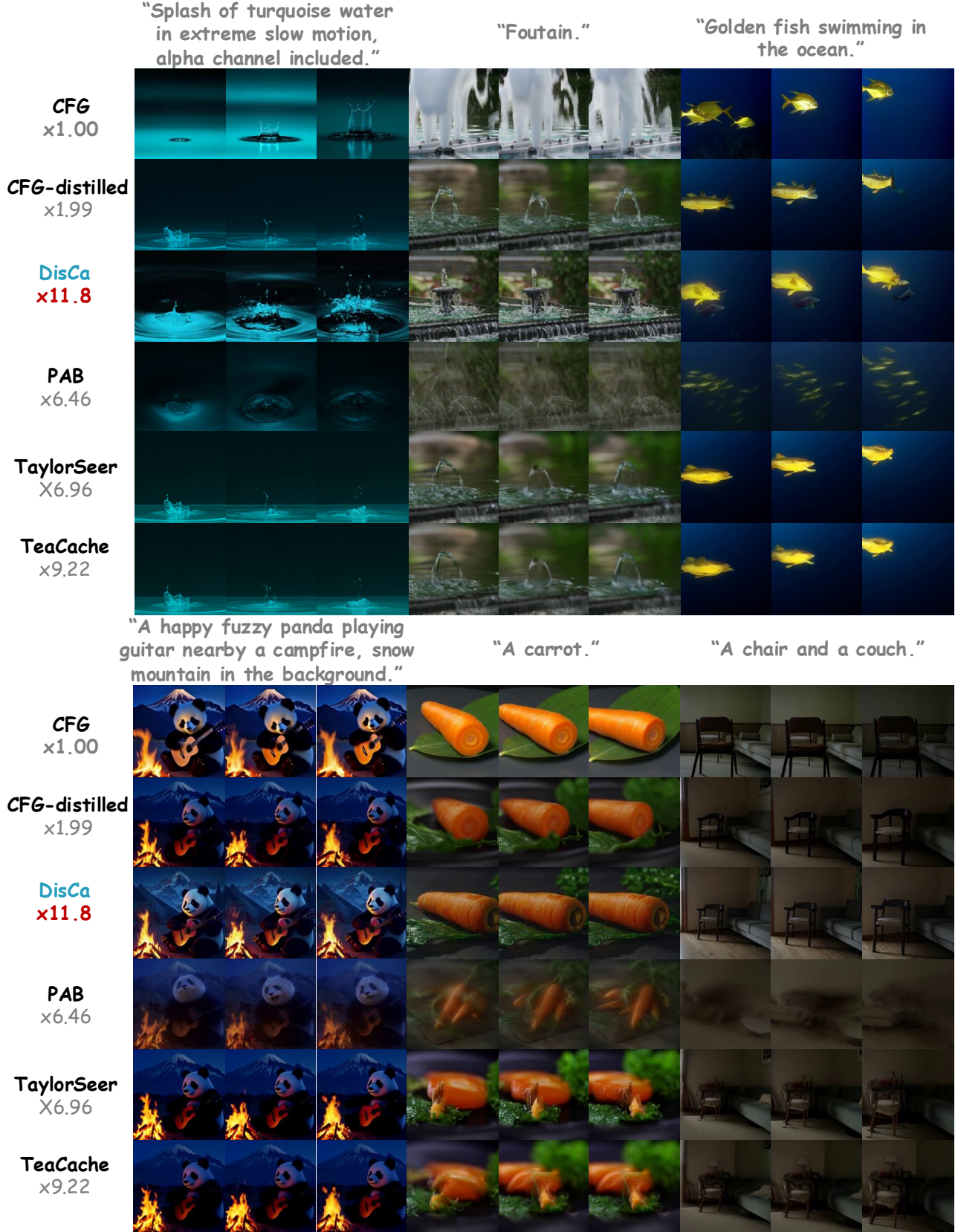


Figure 7. **More visualization examples for HunyanVideo.** The numerous examples clearly demonstrate that the proposed **DisCa** not only significantly surpasses previous acceleration schemes in terms of speed but also achieves *immense advantages across multiple criteria, including structural semantics, detail fidelity, temporal consistency, adherence to physical plausibility, and aesthetic quality.*

6.4.2. Cache Architecture Effects Actual Latency

Prior works on feature caching have largely overlooked the relationship between the caching architecture and the discrepancy between theoretical and practical speedups. In this work, we analyze this gap and discuss its implications under the Distributed Parallel conditions.

As shown in Table 4, we calculated the corresponding floating point operations (FLOPs) for each acceleration method and estimated their theoretical speedup ratio by referencing the FLOPs compression, which is then compared against the measured speedup ratio in Table 2.

As in Table 4, the theoretical and actual speedup ratios for CFG Distilled, MeanFlow, and Restricted MeanFlow are extremely close. Among the cache acceleration methods, the theoretical and actual speedup ratios for TeaCache and Δ -DiT are also well aligned. However, schemes such as PAB, FORA, and TaylorSeer exhibit a significant difference between their theoretical and actual speedup ratios. The closeness of the theoretical and actual speedup ratios for CFG Distilled, MeanFlow, and Restricted MeanFlow is obviously reasonable because they can be understood as simply reducing the number of computation steps, while the discrepancy observed among the cache acceleration methods, however, is worth considering.

Those with a significant difference between theoretical and actual speedup in Table 4, PAB, FORA, and TaylorSeer, all have a multi-layer cache structure. Specifically, they are multi-layer feature caching schemes that cache the output of each neural network layer individually, retaining the residual structure of the DiT Block to utilize richer features for computation. They prepare a set of cached tensors for every DiT Block: for PAB, it is the output of the attention calculation; for FORA, it is the output of both the attention and MLP calculations; and for TaylorSeer, it additionally includes their multi-order derivatives.

As mentioned above, these schemes impose a particularly large VRAM overhead on the device. Furthermore, such a multi-layer cache structure generates frequent memory accesses during the cache step, and reusing these caches leads to multiple, albeit minor and especially sparse, calculations. In previous scenarios where sequence parallelism was not enabled, computational resources on the device were tight, and these memory accesses and sparse computations were optimized by low-level hardware libraries. Therefore, the extra overhead, though present, was not severe enough to warrant action.

However, with the sequence parallelism technique enabled here, computational resources become relatively abundant. As a result, these sparse memory accesses and computations are not fully optimized by the low-level hardware libraries and the GPU device, leading to unexpectedly greater time consumption. In contrast, TeaCache and Δ -DiT generate only one memory access and one simple,

reused extra computation during a single cache-step inference, so their additional overhead is almost negligible.

Summary: *The cache structure is particularly critical in high-resolution, long-sequence video generation scenarios. It not only determines VRAM overhead but also significantly impacts computational efficiency in a parallel environment. Clearly, only reusing the cache in the final layer, instead of a complex multi-layer cache structure, is more appropriate.*

The proposed DisCa employs this single-final-layer-cache structure. Although the introduction of the additional small neural network predictor results in higher extra computation during the cache step than methods like TaylorSeer, which use simple calculations for prediction, this computational overhead remains negligible compared to a complete DiT inference. Furthermore, because the predictor calculation introduced by DisCa is inherently *highly parallelized and imposes low memory access pressure*, it can achieve an acceleration ratio of up to **11.8 \times** , with the difference from the theoretical acceleration even in the margin of error.

6.5. More Visualization Results

In this section, we provide additional visualization examples to further substantiate the superior improvement achieved by the proposed **DisCa** compared to previous acceleration schemes, as shown in Figure 7.

7. Detailed Algorithms

In this section, we present detailed algorithms as pseudo-code for the aforementioned CFG Distillation, Restricted MeanFlow Distillation, and Generative Adversarial Training process for the Predictor to facilitate understanding.

Algorithm 1 CFG distillation

Input: max and min cfg scale g_{max}, g_{min} ,
 - data-noise-text pairs $\{x_0, \epsilon, c\}_i$,
 - CFG Model \mathcal{M}^{CFG} .
Init: CFG Distilled Model $\mathcal{M}_\theta^* = \mathcal{M}^{CFG}$.

- 1: **while** Training **do**
- 2: Sample $t \sim U(0, 1)$, $g \sim U(g_{min}, g_{max})$.
- 3: Sample $x_t = (1 - t) \cdot x_0 + t \cdot \epsilon$.
- 4: Compute $v_c = \mathcal{M}^{CFG}(x_t, t, c)$.
- 5: Compute $v_{uc} = \mathcal{M}^{CFG}(x_t, t, None)$.
- 6: Compute $v_{target} = g \cdot v_c + (1 - g) \cdot v_{uc}$.
- 7: Compute $v_\theta = \mathcal{M}_\theta^*(x_t, t, c)$.
- 8: Compute $loss = \|v_\theta - v_{target}\|_2^2$.
- 9: $loss.backward()$, $optimizer.step()$
 # Loss backward & optimize parameter θ .
- 10: **end while**
- 11: **return** CFG Distilled Model \mathcal{M}_θ^* .

Algorithm 2 Restricted MeanFlow distillation

Input: data-noise pairs $\{x_0, \epsilon\}_i$,
- CFG distilled \mathcal{M}^* ,
- Restrict factor \mathcal{R} .
- *# text info c is omitted for simplification.*
Init: Restricted MeanFlow model $\mathcal{M}_\theta = \mathcal{M}^*$

- 1: **while** Training **do**
- 2: Sample $t, r = \text{sample_t_r}(\mathcal{R})$:
 # Sampling in Restricted MeanFlow.
 # Sample $\mathcal{I} \sim U(0, \mathcal{R})$.
 # Sample $t \sim U(0, 1)$.
 # Compute $r = \max(0, t - \mathcal{I})$.
- 3: Sample $x_t = (1 - t) \cdot x_0 + t \cdot \epsilon$.
- 4: Compute $v = \mathcal{M}^*(x_t, t)$.
- 5: Compute $u, du/dt = \text{jvp}(\mathcal{M}_\theta, (x_t, r, t), (v, 0, 1))$
- 6: Compute $u_{tgt} = v - (t - r) \cdot du/dt$.
- 7: Compute $\text{loss} = \|u - \text{stopgrad}(u_{tgt})\|_2^2$.
 # No gradient backward go through u_{tgt} .
- 8: $\text{loss.backward}()$, $\text{optimizer.step}()$
 # Loss backward & optimize parameter θ .
- 9: **end while**
- 10: **return** Restricted MeanFlow Distilled Model \mathcal{M}_θ .

Algorithm 3 Predictor Training

Input: data-noise pairs $\{x_0, \epsilon\}_i$,
- Sampling timestep pairs $\{(t, r)\}_i$,
- Restricted MeanFlow distilled model \mathcal{M} ,
- max cache interval Δ_{max} .
- Features Extractor $\mathcal{F} := \mathcal{M}$,
Init: random initialized Predictor \mathcal{P}_{θ_P} ,
- random initialized Discriminator D_{θ_D} .

- 1: **while** Training **do**
- 2: Sample $\Delta \sim U(0, \Delta_{max})$.
- 3: Compute $(t', r') = \max((0, 0), (t - \Delta, r - \Delta))$.
- 4: Sample $x_t = (1 - t) \cdot x_0 + t \cdot \epsilon$.
- 5: Compute $\mathcal{C} = \mathcal{M}(x_t, r, t)$. *# Initialize Cache*
- 6: Sample $x_{t'} = (1 - t') \cdot x_0 + t' \cdot \epsilon$.
- 7: Compute $u_{pred} = \mathcal{P}_{\theta_P}(\mathcal{C}, x_{t'}, r', t')$.
- 8: Compute $u_{tar} = \mathcal{M}(x_{t'}, r', t')$.
- 9: Compute $x_{t''}^{pred} = x_{t'} - (t' - r') \cdot u_{pred}$.
- 10: Compute $x_{t''}^{tar} = x_{t'} - (t' - r') \cdot u_{tar}$.
- 11: Define $(t'', r'') = (r', r' - (t'' - r''))$.
- 12: Compute $\mathcal{L}_P = \|u_{pred} - u_{tar}\|_2^2 + \lambda \cdot \max(0, 1 - \mathcal{D} \circ \mathcal{F}(x_{t''}^{pred}))$,
- 13: $\mathcal{L}_P.backward()$, $\text{optimizer_P.step}()$
- 14: Compute $\mathcal{L}_D = \max(0, 1 - \mathcal{D} \circ \mathcal{F}(x_{t''}^{pred})) + \max(0, 1 + \mathcal{D} \circ \mathcal{F}(x_{t''}^{tar}))$.
- 15: $\mathcal{L}_D.backward()$, $\text{optimizer_D.step}()$
 # Loss backward & optimize parameter θ_P, θ_D .
- 16: **end while**
- 17: **return** Restricted MeanFlow Distilled Model \mathcal{M}_θ .
